Snow Water Equivalent retrieval and InSAR Coherence modeling using L-band Lutan-1 data

Jingtian Zhou[1],Yang Lei[1], Jinmei Pan[1], Chuan Xiong[2], Jiancheng Shi[1], Zhenzhan Wang[1], Anmin Fu[3]

[1] National Space Science Center, Chinese Academy of Sciences;

[2]Southwest Jiaotong University, China;

[3]National Forestry and Grass Administration, China;

Contact: zhoujingtian@nssc.ac.cn

1. Motivation & Objective

- **The Gap:** L-band InSAR is highly promising for Snow Water Equivalent (SWE) retrieval, yet limited by the lack of short-revisit data and monostatic snow InSAR models.
- **Our Work:** Using the 4/8-day repeat-pass Lutan-1 data over Altay to:
  - Retrieve SWE variations.
  - Optimize + validate the proposed snow InSAR coherence model

Imaging mode	Stripmap1
Polarization	HH or VV
Resolution	3m×3m
Swath width	50km

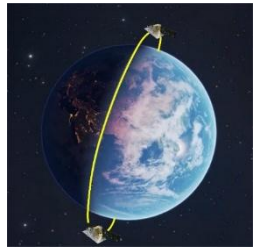

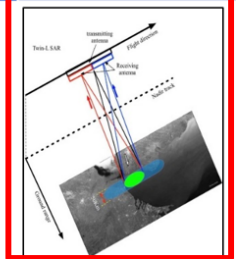

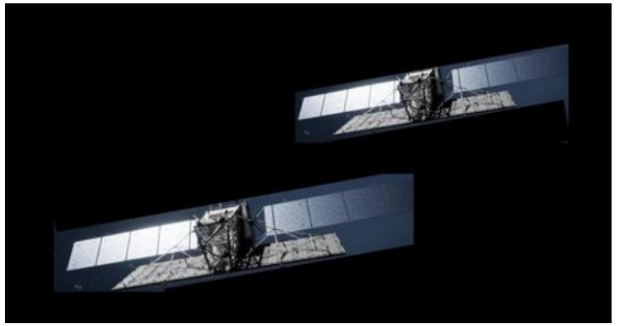

Chinese L-band SAR Constellation (Lutan-1 Mission)

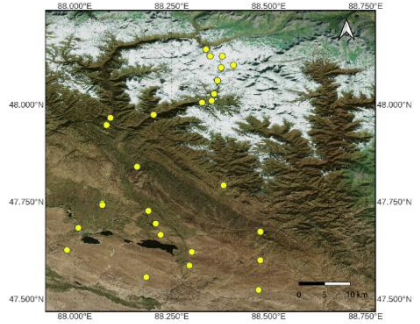

Pictures and in-situ snow sites at Altay

2. Data & Method

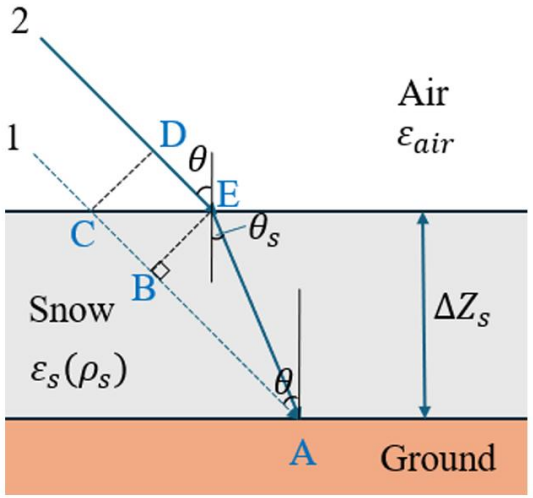

$$\Delta\Phi_s = 2k_i \cdot \frac{\alpha}{2}\left(1.59 + \theta^{5/2}\right) \cdot \Delta\mathrm{SWE}$$

(Guneriussen et al., 2001; Leinss et al., 2015; Zhou et al., 2025)

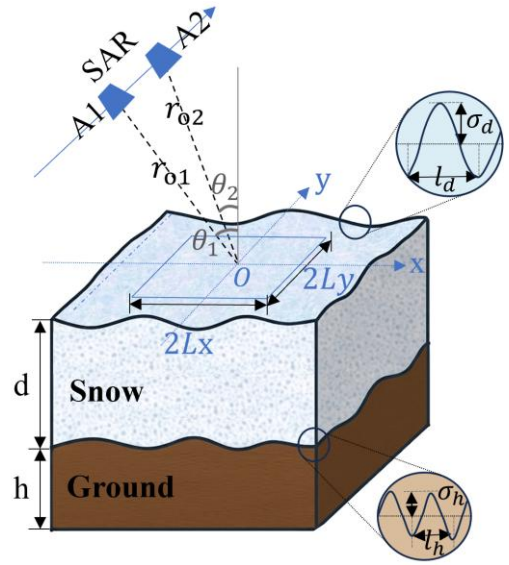

$$\gamma = \frac{\langle S_1 S_2^{*} \rangle}{\sqrt{\langle |S_1|^2 \rangle \langle |S_2|^2 \rangle}} = \frac{\int_{-\infty}^{+\infty}\int_{-\infty}^{+\infty}\int_{-\infty}^{+\infty}\int_{-\infty}^{+\infty} \cdots e^{-2\left(\nu_1^2\sigma_{d1}^2 - 2\nu_1\nu_2 C_{d0}\sigma_{d1}\sigma_{d2} e^{\frac{(x_1-x_2)^2+(y_1-y_2)^2}{l_{dt2}^2}} + \nu_2^2\sigma_{d2}^2\right)+\cdots} dx_1 dx_2 dy_1 dy_2}{\sqrt{\langle |S_1|^2 \rangle \langle |S_2|^2 \rangle}}$$

- **Data:** *Lutan-1 (L-band, 4/8-day revisit)* **+** *Altay In-situ SWE observations*.
- **SWE Retrieval:** Phase-to-SWE conversion **+** Processing procedures
- **Snow InSAR Model:** An InSAR scattering model incorporating spatial heterogeneity of both ground elevation and snow depth.

3. Key Achievements & Future Potential

- **Key Achievements:**
  - **Retrieval:** Achieved RMSE = 9 mm (R=0.48) for 4-day temporal baselines (Dry snow). Heavy snowfall induces severe decorrelation.
  - **Modeling:** Modeled coherence shows a good agreement with observations (R=0.82) after process-based parameter optimization.

- **Findings:** Coherence is highly sensitive to snow depth spatial heterogeneity and density changes

- **Potential:** Demonstrates the operational potential of existing and upcoming short-revisit L-band missions (Lutan-1, ALOS-4, NISAR, ROSE-L).

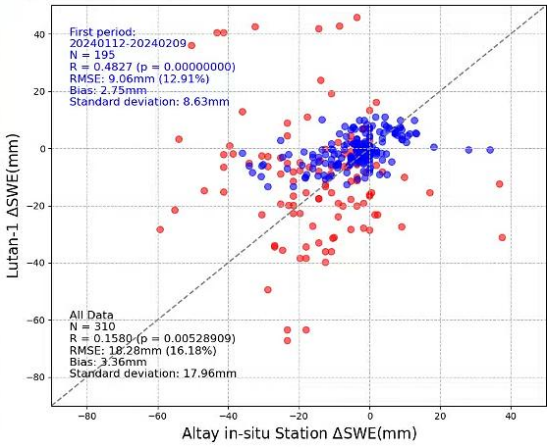

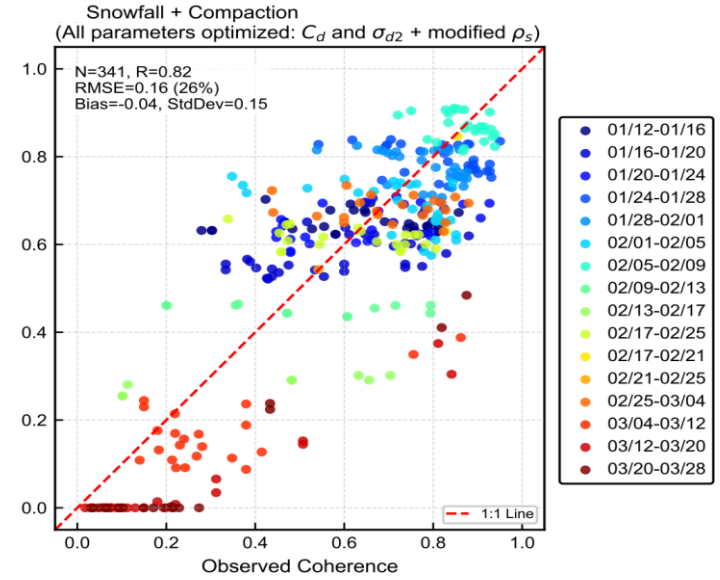

Thank you for your listening!

Contact: zhoujingtian@nssc.ac.cn

Part I: Snow Water Equivalent retrieval using L-band Lutan-1 data

Jingtian Zhou[1],Yang Lei[1], Jinmei Pan[1], Chuan Xiong[2], Jiancheng Shi[1], Zhenzhan Wang[1], Anmin Fu[3]

[1] National Space Science Center, Chinese Academy of Sciences;

[2]Southwest Jiaotong University, China;

[3]National Forestry and Grass Administration, China;

Contact: zhoujingtian@nssc.ac.cn

➢1. Background and Motivation

- **Snow Water Equivalent (SWE):** the depth of water produced if the entire snow column melts

$$SWE = \int_0^{z_s} \rho_s(z)\, dz$$

Why SWE matters?

- **Accurate SWE** information is critical for meteorology, hydrology, and the water cycle.

Current challenge

- However, current remote sensing methods still struggle to provide SWE with the sufficient spatial and temporal resolution required for hydrological applications.

Opportunity

- **Interferometric SAR (InSAR)** offers high spatial resolution and sensitivity to surface changes, providing a new opportunity for retrieving **SWE change** from space.

Snow cover in the Northern Hemisphere
https://www.grida.no/resources/7146

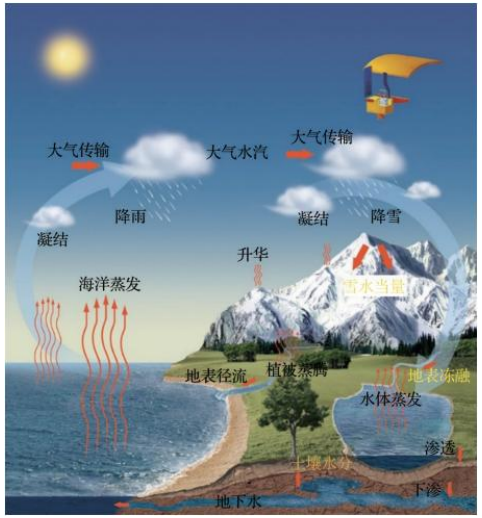

Global Water Cycle
Shi J C,Dong X,Zhao T,et al.WCOM: The Science Scenar-io and Objectives of a Global Water Cycle Observation Mission，2014

Tarricone, Jack, et al. "A Review of Interferometric Synthetic Aperture Radar (InSAR) and Phase-Based Techniques for Monitoring Seasonal Snow." Authorea Preprints (2025).

2.1 Study Area

Altay region in China

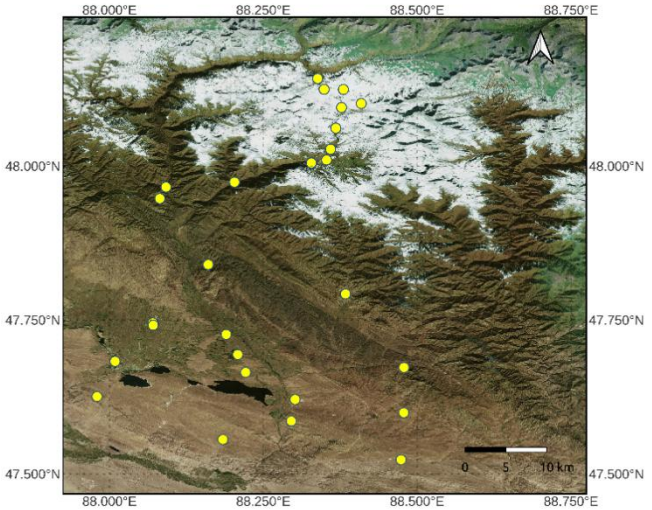

In situ snow sites at Altay

- Annual Snow Depth: Mean ~40 cm; Peak >70 cm (Dai et al., 2022).
- Typical Snow Density: 200 kg/m³ (Yue et al., 2017).
- Snow Cover Duration: 5–6 months (Sept/Oct to April/May).

2.2 Theory for InSAR-based SWE Retrieval

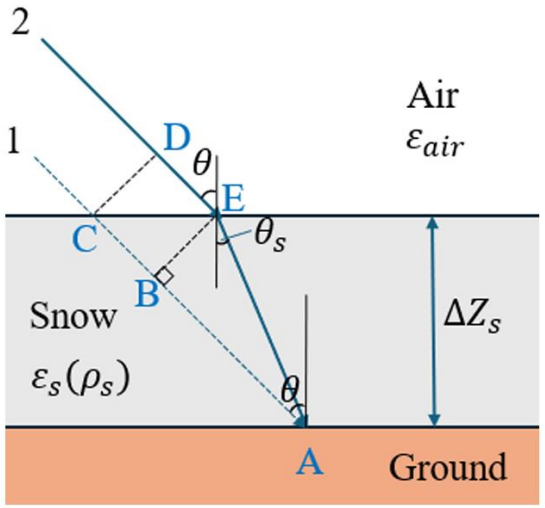

$$\Delta\Phi_s = 2k_i \cdot \frac{\alpha}{2}\left(1.59 + \theta^{5/2}\right) \cdot \Delta\mathrm{SWE}$$

(Guneriussen et al., 2001; Leinss et al., 2015; Zhou et al., 2025)

- **Long wavelength**
  - high coherence: vegetation area or long temporal baseline
- **Short repeat cycle**
  - high coherence: snowfall process
- **Long time series**
  - high precision: atmospheric influence

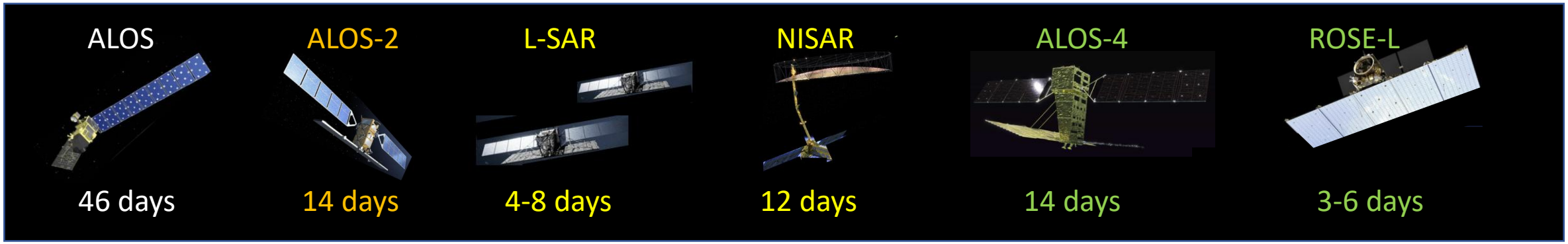

2.3 Lutan-1 Mission

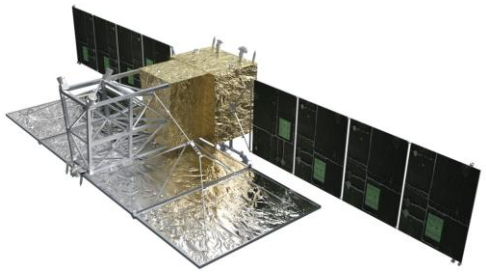

bistatic

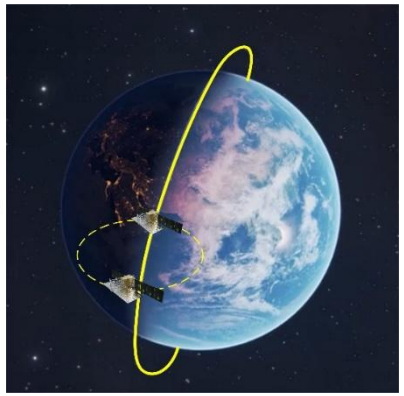

repeat-pass

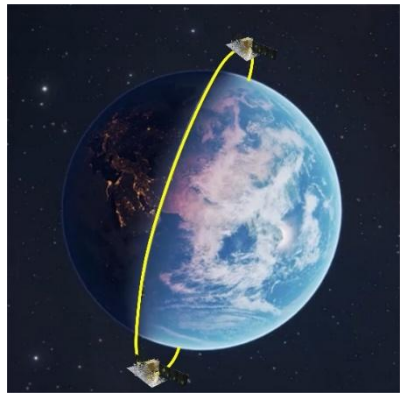

Frequency: 1.26 GHz

Mission Specifications	
constellation	Repeat-pass (primary), bistatic (secondary)
Orbit type	Sun-synchronous
Orbit alitude	607.05km
Latitude limits	±85°
Imaging mode	6
Polarization	Full-pol
Repeat cycle	8 days (single satellite), 4 days (twin satellites)
Inclination	97.8°
Precise Orbit Control	10 cm
National coverage cycle	44 days

Imaging mode	Stripmap1	Stripmap2	Stripmap3	Stripmap4	Stripmap5	ScanSAR
Polarization	HH or VV	HH or VV	HH + HV or VV + VH	HH + HV + VV+ VH	HH or VV	HH or VV
Resolution	**3m×3m**	**12m×12m**	**3m×3m**	**6m×6m**	**24m×24m**	**30m×30m**
Swath width	**50km**	**100km**	**50km**	**30km**	**160km**	**400km**

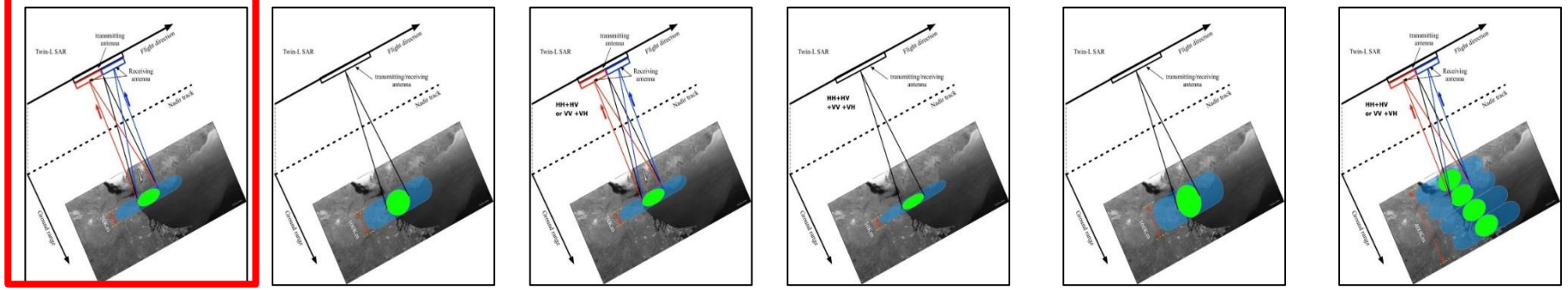

2.4 Lutan-1 InSAR Data Processing Methods

Lutan-1 data in 2024 over Altay

	Date (month, dd)	Temporal baseline (days)	Total images
Start	Jan., 12	4	8
End	Feb., 9		
Start	Feb.,17	8	6
End	Mar., 28		

Processing chain

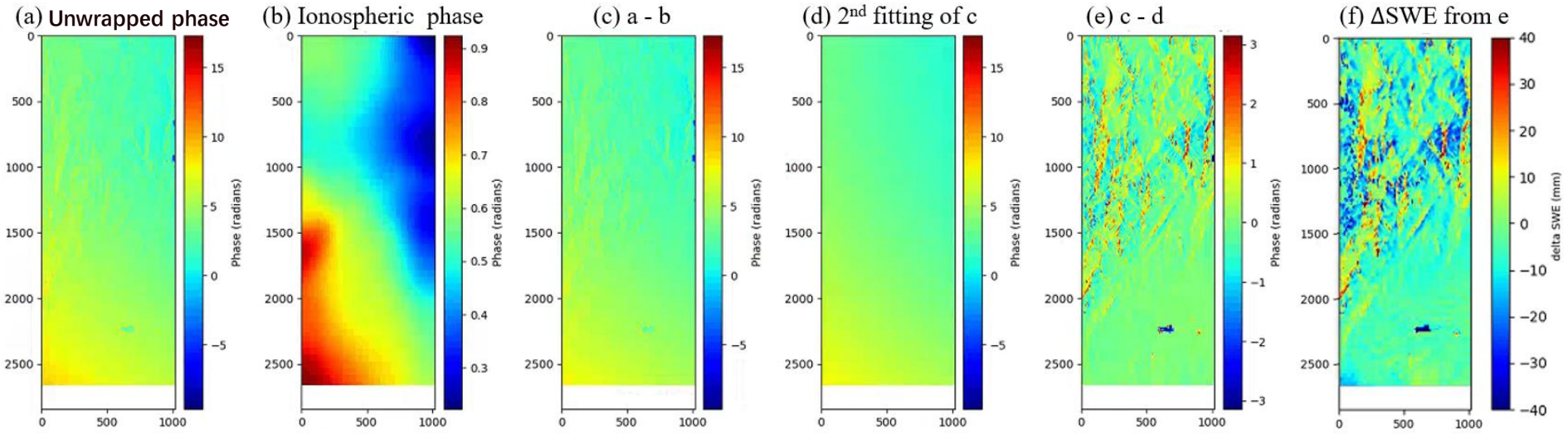

3.1 Results and Analysis: Lutan-1

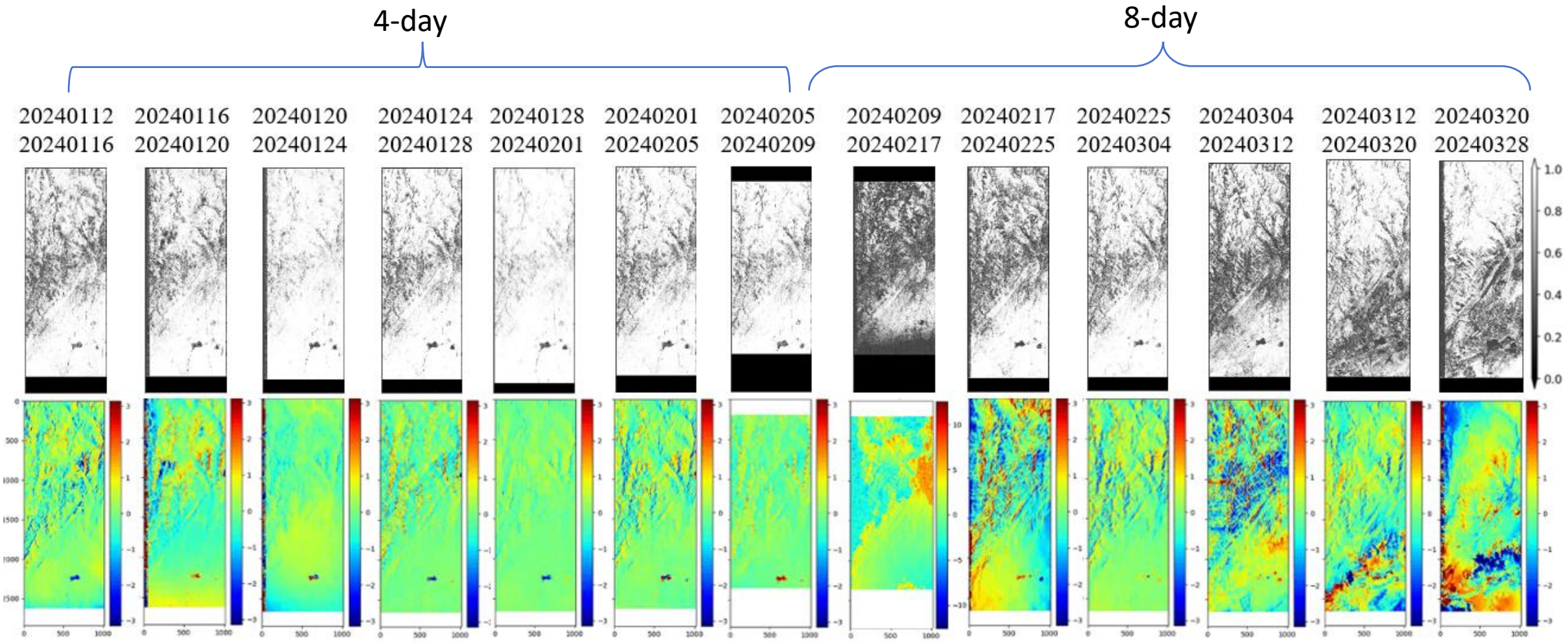

Coherence and unwrapped phase

after interferometric processing of Lutan-1's data over Altay in 2024

3.2 Validation of Lutan-1 SWE Retrieval

Snow & Temperature Variation (Altay Station)

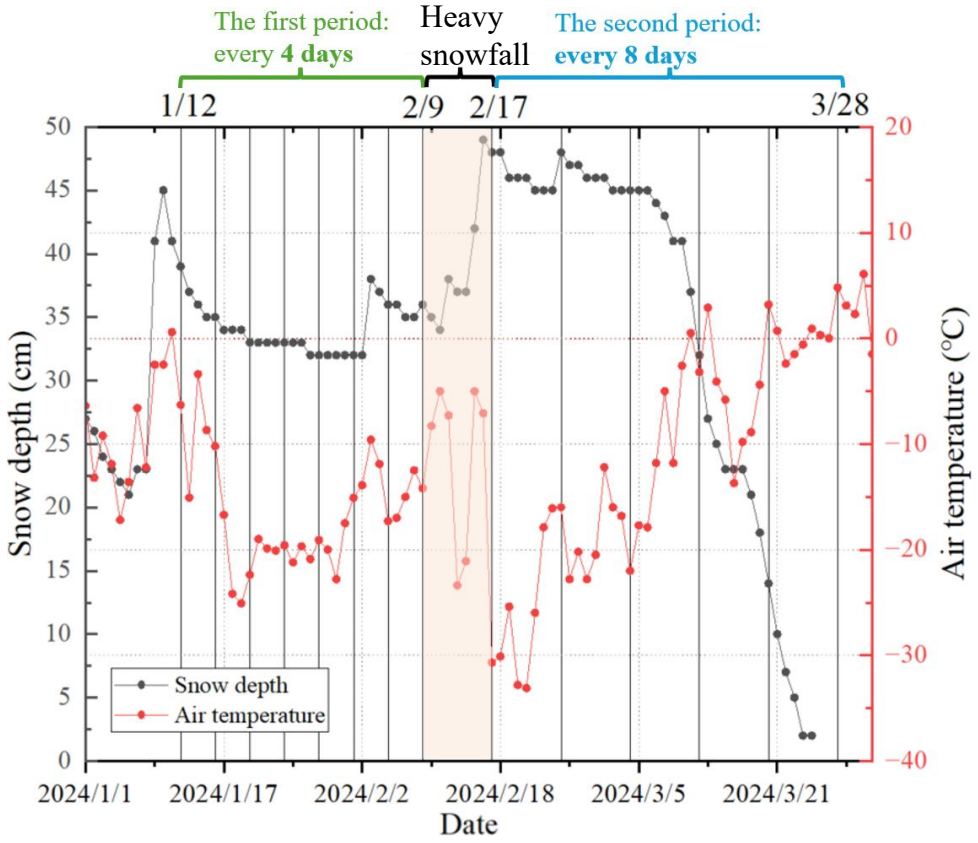

In-situ vs. Lutan-1 InSAR ΔSWE

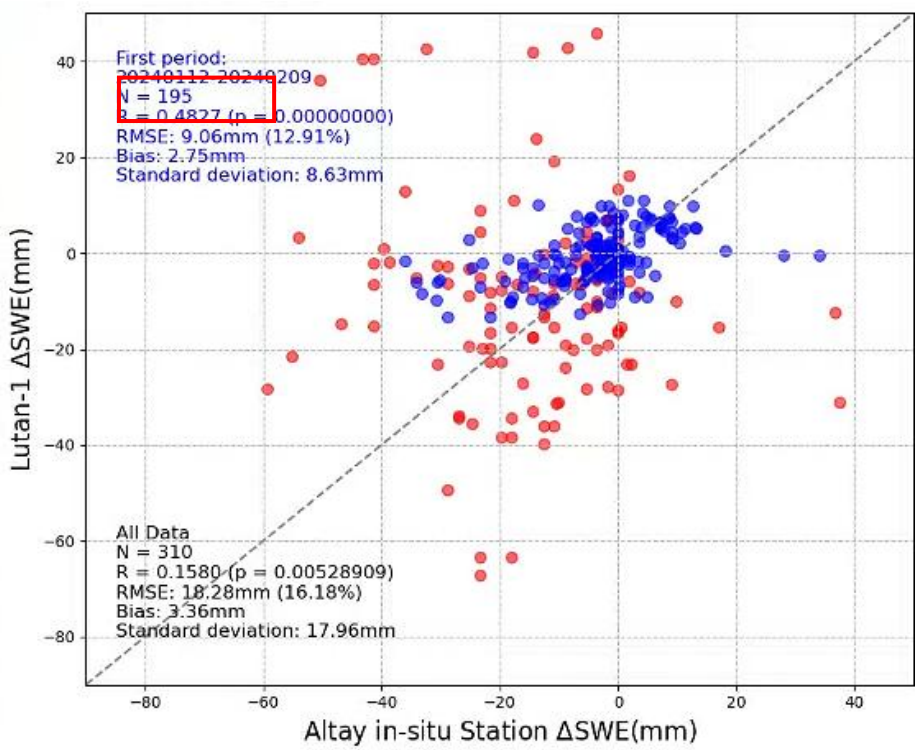

Performance (4-day Dry Snow):

- **RMSE:** 9 mm
- **R:** 0.48
- **Spatial Resolution:** 60 m

Zhou, J., Lei, Y., Pan, J., Xiong, C., Shi, J., Wang, Z., & Fu, A. (2025, August). Snow Water Equivalent Retrieval Over Altay Using Spaceborne Repeat-pass Lutan-1 L-band InSAR. In *IGARSS 2025-2025 IEEE International Geoscience and Remote Sensing Symposium* (pp. 2387-2391). IEEE.

3.3 Results and Analysis: Sentinel-1 SWE retrieval

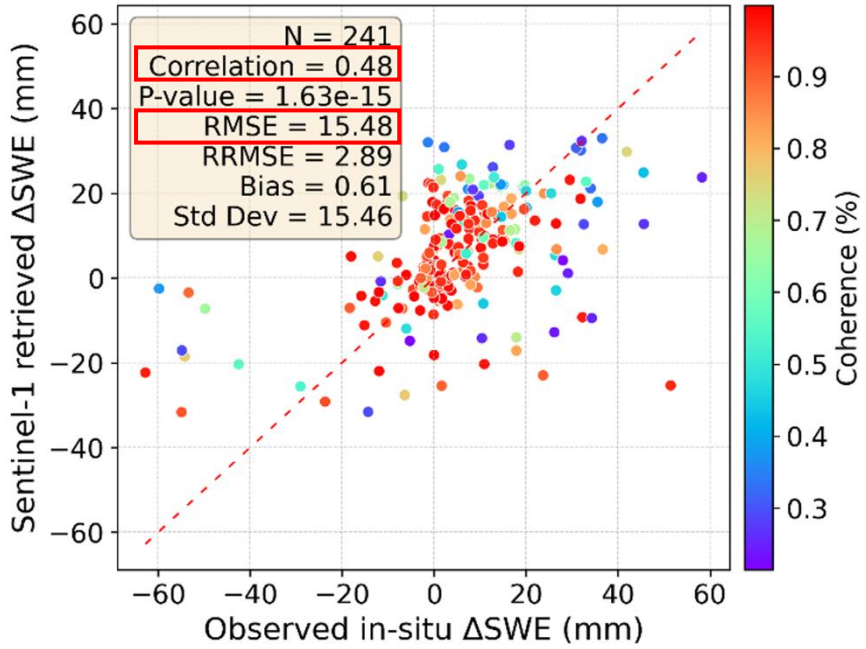

Xiaodonggou station

Hongfuqiao station

"Snow Water Equivalent Retrieval and Analysis Over Altay Using 12-Day Repeat-Pass **Sentinel-1** Interferometry". ***The Cryosphere*** *(2025).*

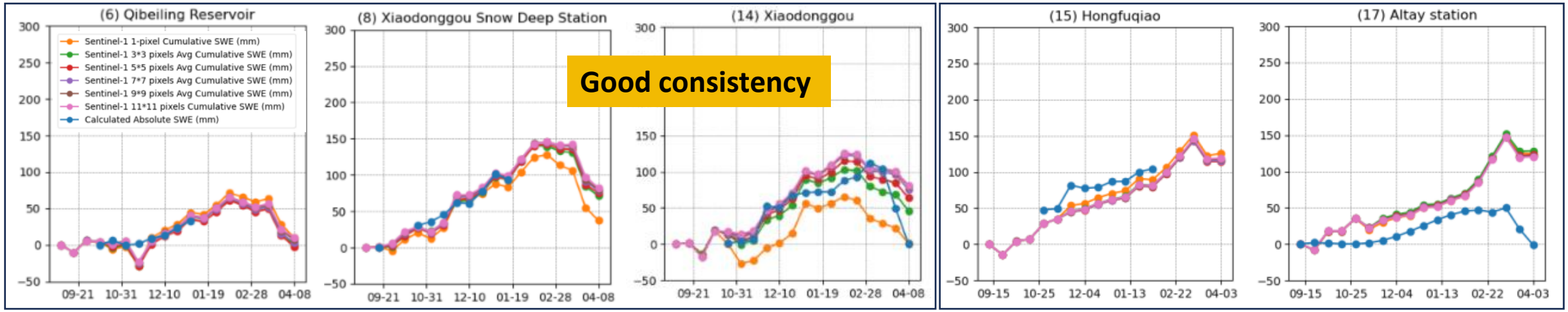

2019-2020

2020-2021

Part II: **Snow InSAR Coherence modeling** using L-band Lutan-1 data

Jingtian Zhou[1],Yang Lei[1], Jinmei Pan[1], Chuan Xiong[2], Jiancheng Shi[1], Zhenzhan Wang[1], Anmin Fu[3]

[1] National Space Science Center, Chinese Academy of Sciences;

[2]Southwest Jiaotong University, China;

[3]National Forestry and Grass Administration, China;

Contact: zhoujingtian@nssc.ac.cn

1. Snow InSAR Coherence Model

S_1 and S_2 are radar signals observed from the same resolution cell in two separate observations.

$$S_1 = \int_{-\infty}^{+\infty}\int_{-\infty}^{+\infty} \Gamma(\vec{r}_1) P_{TR}(\vec{r}_1) e^{-jk2(r_{o1}+x_1\sin\theta_1 - h_1(x_1,y_1)\cos\theta_1)} e^{-jk2\left(\cos\theta_1 - \sqrt{\varepsilon_1 - \sin^2\theta_1}\right)d_1(x_1,y_1)} dx_1 dy_1$$

$$S_2 = \int_{-\infty}^{+\infty}\int_{-\infty}^{+\infty} \Gamma(\vec{r}_2) P_{TR}(\vec{r}_2) e^{-jk2(r_{o2}+x_2\sin\theta_2 - h_2(x_2,y_2)\cos\theta_2)} e^{-jk2\left(\cos\theta_2 - \sqrt{\varepsilon_2 - \sin^2\theta_2}\right)d_2(x_2,y_2)} dx_2 dy_2$$

$$\langle S_1 S_2^* \rangle = e^{-jk2(\vec{r}_{o1}-\vec{r}_{o2})} \int_{-\infty}^{+\infty}\int_{-\infty}^{+\infty}\int_{-\infty}^{+\infty}\int_{-\infty}^{+\infty} P_{TR}(\vec{r}_1) P_{TR}(\vec{r}_2) e^{-jk2(x_1\sin\theta_1 - x_2\sin\theta_2)} \langle e^{jk2(h_1\cos\theta_1 - h_2\cos\theta_1)} \rangle \langle e^{-jk2((cos\theta_1 - \sqrt{\varepsilon_1 - \sin^2\theta_1})d_1 - (cos\theta_2 - \sqrt{\varepsilon_2 - \sin^2\theta_2})d_2)} \rangle dx_1 dx_2 dy_1 dy_2$$

$$= e^{jk2(\vec{r}_{o2}-\vec{r}_{o1})} e^{jk2\left(\cos\theta_1\bar{h}_1 - \cos\theta_2\bar{h}_2\right)} e^{j\left(-2\nu_1\bar{d}_1 + 2\nu_2\bar{d}_2\right)} \int_{-\infty}^{+\infty}\int_{-\infty}^{+\infty}\int_{-\infty}^{+\infty}\int_{-\infty}^{+\infty} e^{-2k^2\left(\cos^2\theta_1\sigma_{h1}^2 - 2\cos\theta_1\cos\theta_2 C_{h12} + \cos^2\theta_2\sigma_{h2}^2\right)} e^{-2\left({\nu_1}^2\sigma_{d1}^2 - 2\nu_1\nu_2 C_{d12} + {\nu_2}^2\sigma_{d2}^2\right)}$$

$$\operatorname{sinc}\left(\frac{x_1}{L_x}\right)\operatorname{sinc}\left(\frac{y_1}{L_y}\right)\operatorname{sinc}\left(\frac{x_2}{L_x}\right)\operatorname{sinc}\left(\frac{y_2}{L_y}\right) e^{-jk2(x_1\sin\theta_1 - x_2\sin\theta_2)} dx_1 dx_2 dy_1 dy_2$$

Γ: Complex backscatter coefficient, assumed to be 1

P_{TR}: SAR point target response

$\bar{h}$: Average ground elevation

$\bar{\mathrm{d}}$: Average snow depth

$$\nu_i = k\left(\cos\theta_i - \sqrt{\varepsilon(\rho)_{1i} - \sin^2\theta_i}\right)\bar{d}_{1i}$$

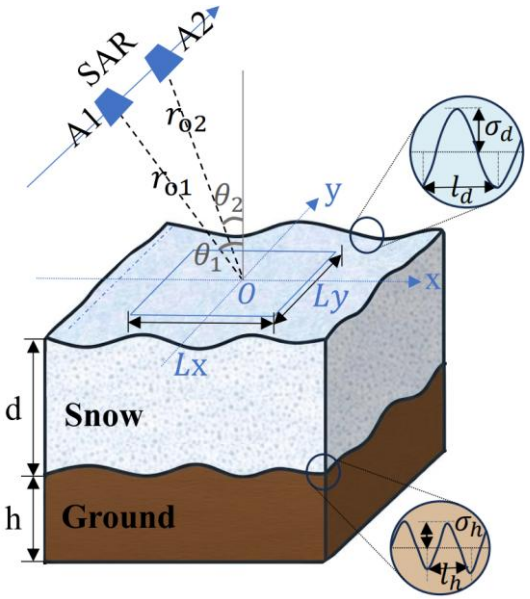

Interferometric coherence

$$\gamma = \frac{\langle S_1 S_2^* \rangle}{\sqrt{\langle |S_1|^2 \rangle \langle |S_2|^2 \rangle}} = \frac{\int_{-\infty}^{+\infty}\int_{-\infty}^{+\infty}\int_{-\infty}^{+\infty}\int_{-\infty}^{+\infty} \cdots e^{-2\left(\nu_1^2\sigma_{d1}^2 - 2\nu_1\nu_2 C_d\sigma_{d1}\sigma_{d2} e^{\frac{(x_1-x_2)^2+(y_1-y_2)^2}{l_{dh2}^2}} + \nu_2^2\sigma_{d2}^2 + \cdots\right)} dx_1 dx_2 dy_1 dy_2}{\sqrt{\langle |S_1|^2 \rangle \langle |S_2|^2 \rangle}}$$

σ_{d} : Snow depth standard deviation

l_{d} : Snow depth correlation length

σ_{h} : Ground elevation standard deviation

l_h : Ground elevation correlation length

C_{d}: Peak coefficient of snow cross-correlation function

2. Impact of Process-Driven Parameters on Coherence

① Snowfall

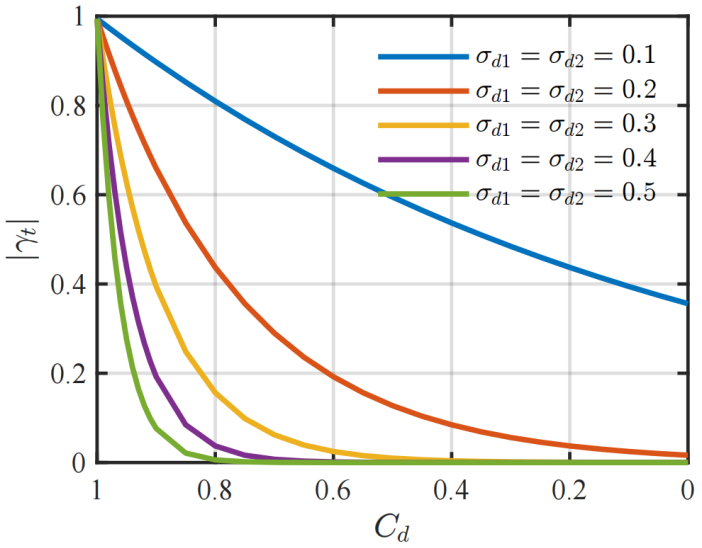

② Snow Compaction

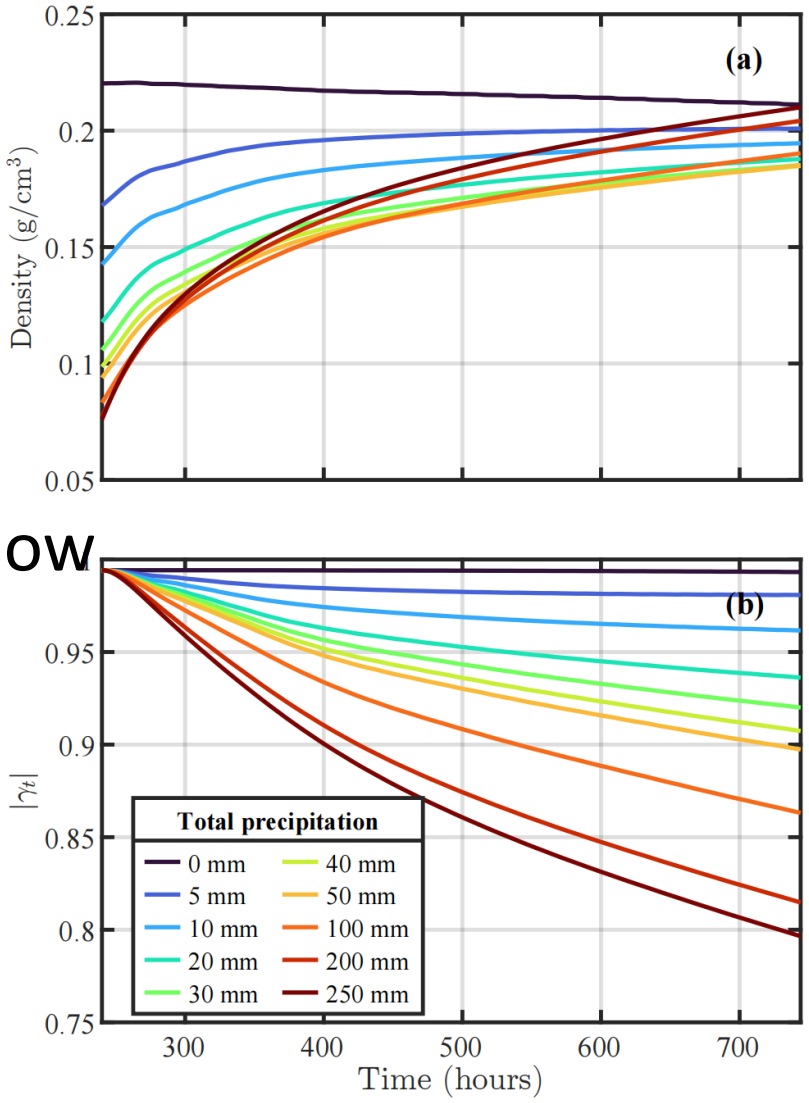

③ Wind-redistributed Snow

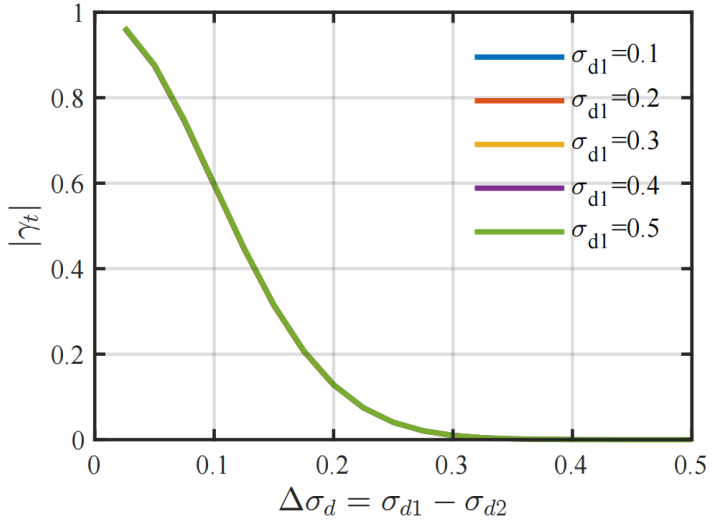

- **(1) Snowfall Process:** Changes in model parameters C_d and σ_d significantly impact coherence.
- **(2) Compaction Process:** Compaction drives variations in both **density** and coherence across different initial snowfall states.
  - **Density** changes dominate the impact on coherence.
- **(3) Wind-blown Snow:** Complete decorrelation occurs when wind-driven changes in snow depth standard deviation exceed 0.3 m.

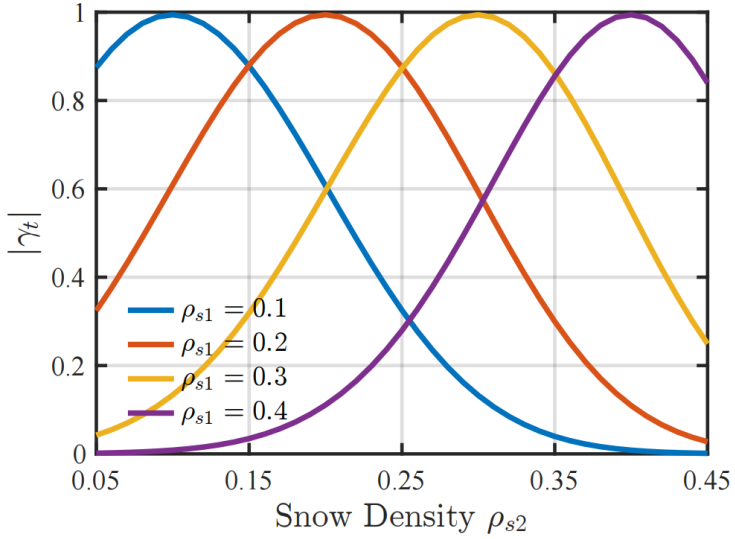

3. Process-Based Parameter Optimization Scheme

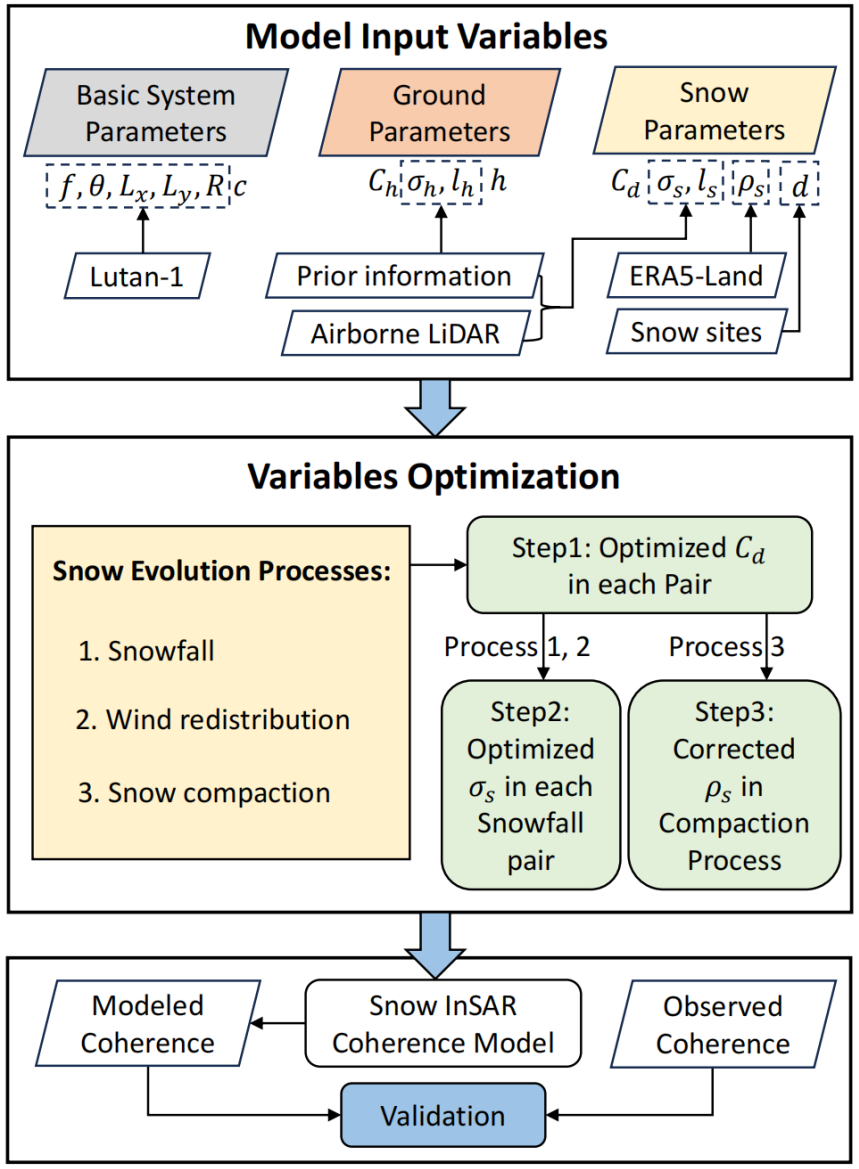

Global optimized parameter scheme

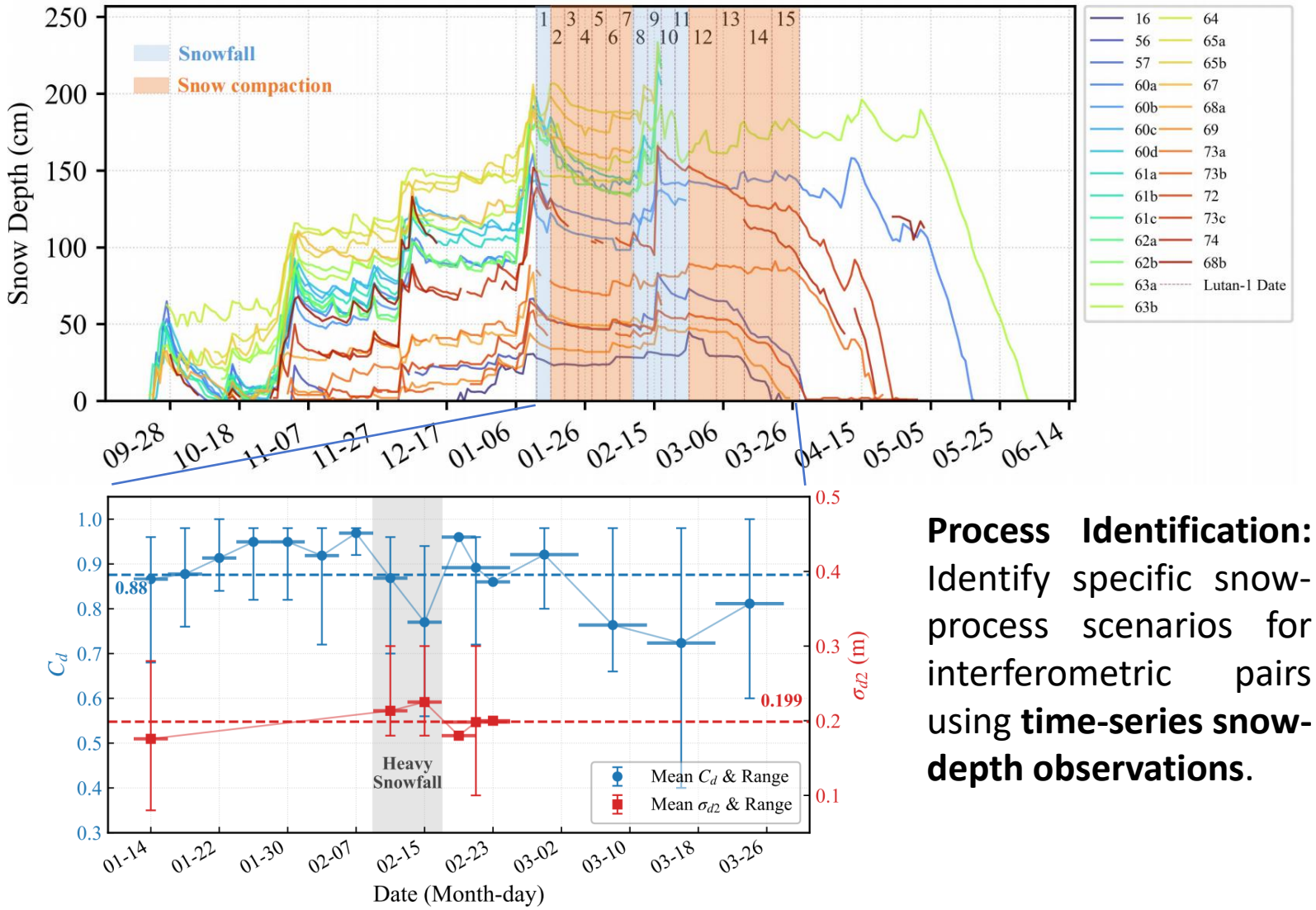

Process Identification: Identify specific snow-process scenarios for interferometric pairs using **time-series snow-depth observations**.

Targeted Optimization: Perform process-specific parameter optimization based on the identified snow processes.

4. Validation of Simulated Coherence against Observations

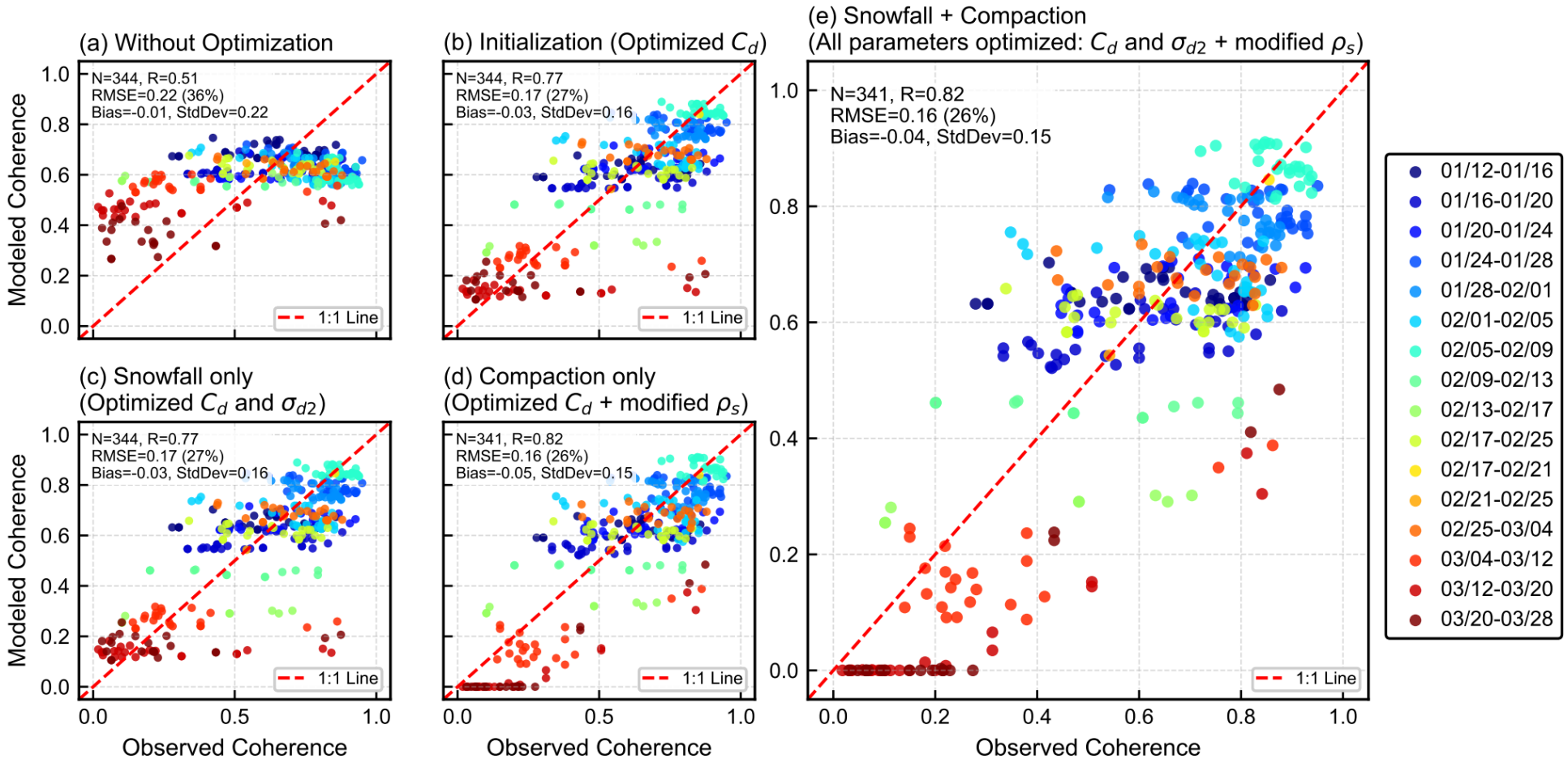

- **Initial vs. All Optimized:** Direct input of measured parameters yields $R = 0.5$ (a). After parameter optimization, accuracy significantly improves to $R = 0.8$ (e).
- **Key Drivers:** Optimized C_{d} strongly enhances simulation results $R = 0.77$ (b).
- **Weak Drivers:** Optimizing σ_{d2} has minimal impact; updating snow density ρ_s yields better performance.
  - *Reason 1:* Likely due to fewer data pairs available for snowfall (associated with σ_{d2}) compared to the compaction process.
  - *Reason 2:* May also reflect the high spatial heterogeneity of RMS height σ_{d2} in real scenarios, limiting the effectiveness of a global σ_{d2} value.

Submitted to IEEE TGRS, 2026

Thank you! Any questions?

Contact: zhoujingtian@nssc.ac.cn